

Technical Report Documentation Page

1. Report No. SWUTC/03/167108-1		2. Government Accession No.		3. Recipient's Catalog No.	
4. Title and Subtitle Modeling the Pneumatic Subsystem of a S-cam Air Brake System		5. Report Date July 2003		6. Performing Organization Code	
		8. Performing Organization Report No. Report 167108		10. Work Unit No. (TRAIS)	
7. Author(s) Shankar C. Subramanian, Swaroop Darbha and K. R. Rajagopal		11. Contract or Grant No. 10727		13. Type of Report and Period Covered	
9. Performing Organization Name and Address Texas Transportation Institute Texas A&M University System College Station, Texas 77843-3135		14. Sponsoring Agency Code		15. Supplementary Notes Supported by general revenues from the State of Texas.	
		12. Sponsoring Agency Name and Address Southwest Region University Transportation Center Texas Transportation Institute Texas A&M University System College Station, Texas 77843-3135		16. Abstract <p>The air brake system is one of the critical components in ensuring the safe operation of any commercial vehicle. This work is directed towards the development of a fault-free model of the pneumatic subsystem of the air brake system. This model can be used in brake control and diagnostic applications. Current enforcement inspections are done manually and hence are time consuming and subjective. The long-term objective is to develop a model-based, performance-based diagnostic system that will automate enforcement inspections and help in monitoring the condition of the air brake system. Such a diagnostic system can update the driver on the performance of the brake system during travel and with recent advancements in communication technology, this information can be remotely transferred to the brake inspection teams. The model of the pneumatic subsystem correlates the pressure transients in the brake chamber with the brake pedal actuation force and the brake valve plunger displacement. An experimental test bench was set up at Texas A&M University and the experimental data is used to corroborate the results obtained from the model.</p>	
17. Key Words Modeling, Air Brake Systems, Commercial Vehicles		18. Distribution Statement No restrictions. This document is available to the public through NTIS: National Technical Information Service 5285 Port Royal Road Springfield, Virginia 22161			
19. Security Classif.(of this report) Unclassified		20. Security Classif.(of this page) Unclassified		21. No. of Pages 56	
				22. Price	

Modeling the Pneumatic Subsystem of a S-cam Air Brake System

By

Shankar C. Subramanian
Department of Mechanical Engineering
3123 TAMU
College Station, TX 77843-3123
Phone: (979) 862-8065
Email: shankarram@tamu.edu

Swaroop Darbha
Department of Mechanical Engineering
3123 TAMU
College Station, TX 77843-3123
Phone: (979) 862-2238
Email: dswaroop@mengr.tamu.edu

K. R. Rajagopal
Department of Mechanical Engineering
3123 TAMU
College Station, TX 77843-3123
Phone: (979) 862-4552
Email: kraagopal@mengr.tamu.edu

Report SWUTC/03/167108-1
Project Number 167108

Research Project Title: Modeling the Pneumatic Subsystem of a S-cam Air Brake System

Sponsored by the

Southwest Region University Transportation Center

July 2003

TEXAS TRANSPORTATION INSTITUTE
The Texas A&M University System
College Station, Texas 77843-3135

ABSTRACT

The air brake system is one of the critical components in ensuring the safe operation of any commercial vehicle. This work is directed towards the development of a fault-free model of the pneumatic subsystem of the air brake system. This model can be used in brake control and diagnostic applications. Current enforcement inspections are done manually and hence are time consuming and subjective. The long-term objective is to develop a model-based, performance-based diagnostic system that will automate enforcement inspections and help in monitoring the condition of the air brake system. Such a diagnostic system can update the driver on the performance of the brake system during travel and with recent advancements in communication technology, this information can be remotely transferred to the brake inspection teams. The model of the pneumatic subsystem correlates the pressure transients in the brake chamber with the brake pedal actuation force and the brake valve plunger displacement. An experimental test bench was set up at Texas A&M University and the experimental data is used to corroborate the results obtained from the model.

ACKNOWLEDGEMENTS

The authors recognize that support for this research was provided by a grant from the U.S. Department of Transportation, University Transportation Centers Program to the Southwest Region University Transportation Center which is funded 50% with general revenue funds from the State of Texas. The authors also thank the National Science Foundation for supporting this project under the NSF/USDOT-ICSST grant 0127941. The authors finally thank Mr. Naman Elamin, Dr. Cem Hatipoglu and Mr. Steve Moran of Bendix Commercial Vehicle Systems for providing the necessary hardware and financial support towards this project. The support of Applied Materials in the form of a graduate fellowship for the first author is gratefully acknowledged.

DISCLAIMER

The contents of this report reflect the views of the authors, who are responsible for the facts and the accuracy of the information presented herein. This document is disseminated under the sponsorship of the Department of Transportation, University Transportation Centers Program, in the interest of information exchange. Mention of trade names or commercial products does not constitute endorsement or recommendation for use.

EXECUTIVE SUMMARY

Air brake systems are used in almost all commercial vehicles in the United States and more than 85% of them use S-cam foundation brakes. In an air brake system, compressed air (provided by a compressor) is stored in storage reservoirs and supplied to the brake application valve (treadle valve). The application of the brake pedal by the driver serves to meter out the compressed air to the various brake chambers resulting in the generation of the braking force. In hydraulic brake systems, the pedal force applied by the driver (usually augmented by a vacuum booster) is transmitted through the brake fluid resulting in the application of the foundation brakes on the wheels. Air brakes systems are very sensitive to maintenance and require periodic inspections.

Inspection techniques used for evaluating air brake systems can be broadly classified into visual and performance-based techniques. Visual inspections involve the measurement of the push rod stroke and the thickness of the brake pad lining and checking the brake lines for wear and leaks. Performance-based inspections include the measurement of braking force and torque, vehicle deceleration, stopping distance, brake pad temperature etc. Visual inspection of an air brake system is highly subjective and time consuming whereas performance-based inspections are more objective. The long-term aim of this project is to develop an on-board, model-based, performance-based diagnostic system that would be useful in automating enforcement inspections.

The first step involved in this task is to develop a fault-free model of the air brake system. An air brake system can be broadly divided into a pneumatic subsystem and a mechanical subsystem. This report presents the work carried out towards the development of a fault-free model of the pneumatic subsystem of an air brake system. An experimental test bench was setup at Texas A&M University and experimental data was collected for a wide range of test runs. The model of the pneumatic subsystem is corroborated with this experimental data. This model correlates the pressure transients in the brake chamber with the brake pedal actuation force and the brake pedal plunger displacement. We aim to use this model in brake control and diagnostic applications.

TABLE OF CONTENTS

1 INTRODUCTION	1
1.1 BACKGROUND	1
1.2 AIM AND SCOPE OF THE PROBLEM	3
1.3 ORGANIZATION OF THE REPORT	4
2 AN OVERVIEW OF THE AIR BRAKE SYSTEM	5
2.1 THE PNEUMATIC SUBSYSTEM	5
2.2 THE MECHANICAL SUBSYSTEM	7
3 THE EXPERIMENTAL SETUP	9
4 MODELING THE AIR BRAKE SYSTEM	13
4.1 THE PRIMARY CIRCUIT	14
4.2 THE SECONDARY CIRCUIT	17
4.3 MODELING THE FLUID FLOW	20
5 CORROBORATION OF THE MODEL	29
6 CONCLUDING REMARKS	35
BIBLIOGRAPHY	37

LIST OF FIGURES

2.1 A general layout of the air brake system in trucks	7
2.2 The mechanical subsystem of a S-cam air brake system	8
2.3 A schematic of a drum brake	8
3.1 A schematic of the experimental setup	9
3.2 A view of the experimental setup	10
3.3 Another view of the experimental setup	10
4.1 A sectional view of the E-7 dual circuit valve	13
4.2 The simplified pneumatic subsystem	20
4.3 The brake chamber as the control volume	22
4.4 A sectional view of the brake chamber	24
5.1 Pressure transients at 515 KPa (60 psig) supply pressure – apply phase	30
5.2 Pressure transients at 653 KPa (80 psig) supply pressure – apply phase	30
5.3 Pressure transients at 722 KPa (90 psig) supply pressure – apply phase	31
5.4 Pressure transients at 584 KPa (70 psig) supply pressure – apply and exhaust phases	32
5.5 Pressure transients at 653 KPa (80 psig) supply pressure – apply and exhaust phases	32
5.6 Pressure transients at 722 KPa (90 psig) supply pressure – apply and exhaust phases	33
5.7 Pressure transients at 584 KPa (70 psig) supply pressure – periodic application .	33

LIST OF TABLES

2.1 Components of the pneumatic subsystem	6
3.1 Details of the equipment and transducers used in the experiment	12
5.1 Values of the parameters used in the simulation	29

CHAPTER 1: INTRODUCTION

1.1 BACKGROUND

The brake system is one of the critical components in ensuring the safety of any vehicle on the road. Most tractor-trailer vehicles with a gross vehicle weight rating over 19,000 lb, most single trucks with a gross vehicle weight rating over 31,000 lb, most transit and inter-city buses, and about half of all school buses are equipped with air brake systems [1]. More than 85% of the commercial vehicles operating in the United States use S-cam drum foundation brakes in their air brake system [1]. The performance of air brake systems used in commercial vehicles is very sensitive to maintenance procedures such as the adjustment of the push rod stroke, brake lining replacement, etc. [2]. Malfunctioning brakes are one of the leading mechanical causes of accidents in commercial vehicles. In 1999, among fatal crashes due to mechanical failure, 28.3% were attributed to defects in the brake system [3]. In roadside inspections performed between 1996 and 1999, 29.3% of all the vehicle-related violations among Intrastate carriers and 37.2% of those among Interstate carriers were due to defects in the brake system [4].

Regulations such as the Federal Motor Vehicle Safety Standards (FMVSS) 121 (effective 1973) govern the braking performance of commercial vehicles on roads in the United States. FMVSS 121 specifies a stopping distance criterion and a criterion for lateral vehicle stability, requiring a vehicle to stay within a twelve feet lane when performing a stopping maneuver [5]. Although regular maintenance inspections are carried by truck owners and fleet operators to conform to FMVSS 121, government agencies such as the Office of Motor Carriers conduct enforcement inspections in the interest of public safety. The criteria set by the Commercial Vehicle Safety Alliance (CVSA) guide such enforcement inspections.

Inspection techniques that are used for monitoring the brake system in commercial vehicles can be broadly classified into two categories - visual inspections and performance-based inspections [6]. Visual inspections involve the measurement of the push rod stroke and the thickness of the brake pad lining and checking the brake lines for wear and leaks. Visual inspections are subjective, time and labor intensive and are inconvenient when the vehicles have low ground clearance. Performance-based inspections include the measurement of braking force and torque, vehicle deceleration, stopping distance, brake pad temperature etc. Such inspections are more objective and offer a more effective assessment of the condition of the air brake system. Currently, such inspections are required in Europe and are performed only in certified inspection garages [6]. It is appropriate to point out that, in an appraisal of the future needs of the trucking industry [7], the authors, who represent a broad spectrum of the trucking industry, indicate that equipment users would greatly appreciate the development of a standardized, universal, hand-held diagnostic tool. They also stress the need for improvements in the existing inspection techniques and advise the need for the development of performance-based tools that can be used along with visual inspections.

An air brake system differs from a hydraulic brake system used in passenger vehicles in many ways. The most important difference is the mode of operation - in a hydraulic brake system, the pedal force applied by the driver (augmented usually by a vacuum booster) is transmitted

through the brake fluid resulting in the application of the foundation brakes on the wheels, whereas, in an air brake system, the application of the treadle valve regulates the air supply from a supply reservoir to the brake chamber. As a result, very little sensory feedback is available to the driver of a commercial vehicle when compared to a vehicle with a hydraulic brake system. Another difference between the two braking systems is in the distribution of the braking force between the various axles. In passenger vehicles, the load distribution on the axles varies slightly whereas in commercial vehicles the distribution of the load on the various axles varies significantly depending on whether the vehicle is loaded or unloaded. Typically, commercial vehicle brakes are designed and balanced for the fully loaded condition and this results in excessive braking on some axles when the vehicle is not fully loaded [2]. This problem is compounded by the fact that the U.S. regulations, unlike the European standards, do not directly specify brake force distribution between the various axles [8].

In addition to the S-cam foundation brakes, retarders are being used as supplementary braking mechanisms. We refer to foundation brakes as to those that are mounted on the end of the axle casing and directly act on the wheels when applied. Retarders are supplementary braking mechanisms and they serve to decrease the work load on the foundation brakes thereby increasing the life of the foundation brakes. Some examples of retarders are compression brakes [9], fluid brakes and eddy current brakes [10]. Compression brakes use the kinetic energy of the crankshaft to compress air in the engine cylinders thus providing a retarding action. Eddy current brakes and fluid brakes are usually mounted on the transmission shaft after the gearbox. The main limitation of such retarders is that they can only supplement the foundation brakes and can never replace them completely. This is due to the poor torque output characteristics of the retarders at low vehicle speeds; moreover they cannot provide any braking effort when the vehicle is at rest [10].

The hydraulic brake system has been extensively studied and models for the system have been developed by many authors. Gerdes et al. [11] developed a model for a hydraulic brake system with a vacuum booster. They combined a static valve model with equations of air flow within the booster. Khan et al. [12] used bond graph techniques to develop models for the booster, the master cylinder and the wheel cylinder. In both cases, the authors measured the wheel cylinder chamber pressure as a function of time and attempted to predict the pressure transients with their models.

The air brake system used in commercial vehicles is made up of two subsystems - the pneumatic subsystem and the mechanical subsystem. The pneumatic subsystem includes the compressor, the storage reservoirs, the brake lines, the treadle valve and terminates at the brake chamber. The mechanical subsystem starts from the brake chamber and includes the push rod, the slack adjuster, the S-cam and the brake pads. Thus, it can be seen that developing a model for the air brake system is a complicated process due to the large number of components involved. The majority of the published work on air brake systems relate brake force, vehicle deceleration, brake pad temperature and brake torque as a function of brake chamber pressure and push rod stroke [13,14,15,16]. In most of the experiments, the brake chamber pressure was measured for each application and was correlated with other measurements such as those mentioned above. This is essentially an indication of the characteristics of the mechanical subsystem of the air brake system.

A model for the pneumatic subsystem must be able to predict the pressure transients in the brake chamber as a function of the supply pressure from the reservoir and the pedal force applied by the driver. More recently, Acarman et al. [17] suggested a model to predict the growth of air pressure in the brake chamber of a brake system equipped with an Antilock Braking System (ABS). They used orifice flow equations to model the dynamics of air flow and included the dynamics of a modulator located downstream from the treadle valve. The modulator regulates the pressure of air in the brake chamber depending on the mode of operation as decided by the ABS controller.

1.2 AIM AND SCOPE OF THE PROBLEM

Our aim is to develop a model that can predict the pressure transients in the brake chamber over a wide range of supply pressures and also at partial brake applications. Such a model is highly desirable since, according to [18], almost 97% of typical service brake applications in commercial vehicles are made below 308 KPa (30 psig). We model the pneumatic subsystem so that the pressure transients in the brake chamber can be predicted from the measurements of the pedal force and pedal displacement. The treadle valve is treated as a nozzle and the dynamics of the treadle valve is incorporated into the model. The reason behind this choice is explained in section (4.3).

We have made certain assumptions in the development of the model. We have adopted a lumped parameter approach in modeling both the mechanical components of the valve and the flow of air in the system. We have neglected the viscosity of air and assumed it behaves like an ideal gas. The expansion process in the valve is assumed to be isentropic and a coefficient of discharge used to account for the losses during expansion. We also assume the flow from the valve to the brake chamber to be adiabatic. All the above assumptions are approximations to the real process and the choice of these approximations is vindicated by the fact that the results from the model developed under these assumptions agree well with the experimental data as will be seen later in Chapter (5). This is not to say that the model cannot be improved upon, however a study that treats the various subsystems of the brake system as a continuum, rather than a lumped parameter, is at the present intractable.

Our long-term aim is to develop an on-board, model-based, performance-based diagnostic tool that can be used in inspecting the air brake system. Such a diagnostic tool can frequently update the driver on the performance of the brake system during travel. With recent advancements in communication technology, it is also possible to transfer the diagnostic information remotely to the roadside inspection teams which will reduce the inspection time significantly. This is desirable since, according to [20], the average time required for a typical roadside inspection is around 30 minutes, with approximately half of the time spent on brakes.

The first step in the development of such a diagnostic tool is the development of a fault-free model of the air brake system. In this report, we deal with the modeling of the pneumatic subsystem of the air brake system. The model will be used to correlate the pressure transients with the brake valve plunger displacement and the brake pedal actuation force. The results from the model will be corroborated with the data obtained from the experiments for various test runs. Once a model is developed for the pneumatic subsystem, it can be combined with a model for the

mechanical subsystem to obtain a complete model of the air brake system. A fault-free model of the air brake system will be able to predict the brake chamber pressure, the push rod stroke, the brake torque and the wheel speed from measurements of the brake valve plunger displacement and the brake pedal actuation force. Thus, a fault-free model gives a correlation between the above mentioned variables under normal operating conditions. The use of this fault-free model in the diagnostic system will help in detecting failures in the air brake system whenever they occur.

1.3 ORGANIZATION OF THE REPORT

Chapter 2 presents a description of the pneumatic and mechanical subsystems of the air brake system. A brief description of the experimental facility at Texas A&M University is presented in Chapter 3. We develop the model of the pneumatic subsystem in Chapter 4. Governing equations for both the primary and the secondary circuit are derived followed by the equations describing the flow of air in the system. Chapter 5 deals with the corroboration of the model for various test runs. The model was simulated for each of the experimental test run and the results are compared with the collected experimental data. In Chapter 6 we summarize the results obtained.

CHAPTER 2: AN OVERVIEW OF THE AIR BRAKE SYSTEM

The air brake system is one of the crucial subsystems of a commercial vehicle. The major functions of the air brake system include the following:

- To decelerate the vehicle from a higher velocity and bring it to a complete stop when needed.
- To maintain the speed of the vehicle on a grade during descent.

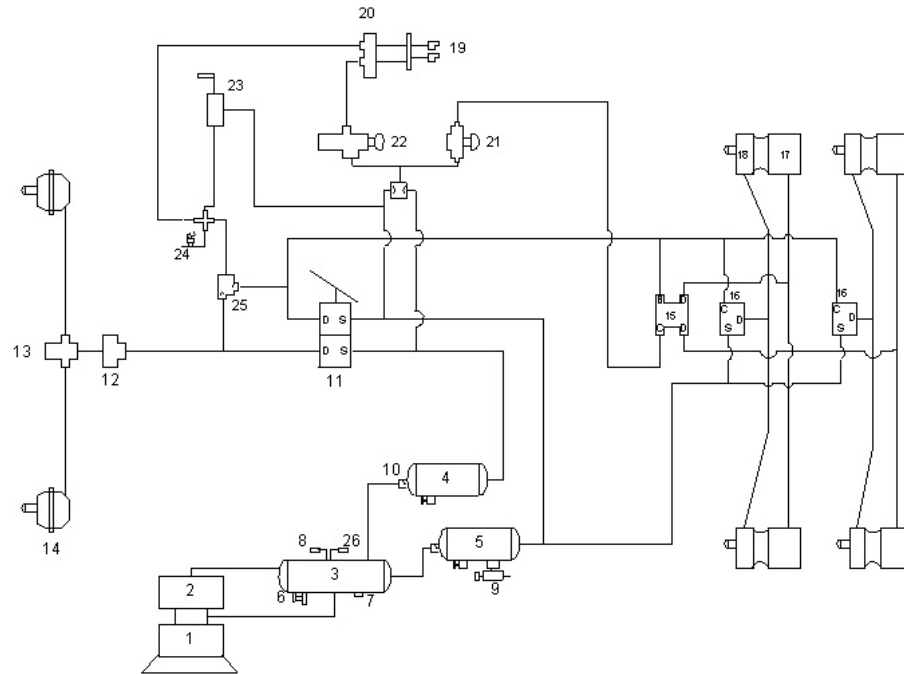
In an air brake system, the compressor acts as the energy source and the brake application valve (treadle valve) acts as the application mechanism. Let us now look at the pneumatic and mechanical subsystems in detail.

2.1 THE PNEUMATIC SUBSYSTEM

A general layout of the pneumatic subsystem in the air brake system of a tractor-trailer is shown in Fig. 2.1. A brief description of some of the components of the pneumatic subsystem is provided in Table (2.1). The compressor charges up the storage reservoirs and the application of the treadle valve modulates the amount of air provided to the brake chambers. Compressed air is supplied from the treadle valve to the various brake chambers through two circuits - the primary circuit and the secondary circuit. The advantage of such an arrangement is that partial braking is possible in the case of failure of one of the two circuits, though the complexity of the system is increased. In trucks, the primary circuit provides compressed air to the rear brakes and the secondary circuit operates the front brakes. Since 1968, federal standards have warranted the use of dual-circuit valve brake systems in cars and other passenger vehicles and since the mid-1970's this requirement was extended to include commercial vehicles with air brake systems [19]. FMVSS 121 spells out the performance standards required for air brake systems and FMVSS 105 provides the standards for hydraulic brake systems.

Table 2.1: Components of the pneumatic subsystem

Component	Description
Compressor	Acts as the energy source providing compressed air.
Storage reservoirs	Store the compressed air and supply it to the treadle and relay valves.
Safety valve	Prevents an excessive pressure build-up in the storage reservoirs.
Drain valve	Removes moisture and contaminants from the air stored in the reservoirs.
Low air pressure switch	Warns the driver when the pressure in the reservoirs falls to around 65-75 psig.
Pressure protection valve	Closes air flow to accessory devices such as air horn, air seat etc., when the pressure in the reservoirs falls below around 65 psig.
Treadle valve	Modulates the amount of air being supplied to the brake chambers.
Quick release valve	Releases the front brakes quickly.
Parking brake control valve	Located in the driver's cab and is used to apply the parking brakes.
Tractor protection valve	Protects the tractor brake system in the case of trailer break-away and/or when there are severe leakages in the brake system.
Trailer brake control valve	Actuates the trailer brakes independent of the tractor brakes and is applied by the driver.



- | | |
|--------------------------------------|--|
| 1 - Air Compressor | 16 - Service Relay Valve |
| 2 - Governor | 17 - Rear Spring Brake Chamber |
| 3 - Wet Supply Reservoir | 18 - Rear Service Chamber |
| 4 - Front System Service Reservoir | 19 - Trailer Couplings |
| 5 - Rear System Service Reservoir | 20 - Tractor Protection Valve |
| 6 - Drain Cock | 21 - Tractor Parking Brake Control Valve |
| 7 - Automatic Drain Valve | 22 - Trailer Supply Valve |
| 8 - Safety Pressure Valve | 23 - Trailer Brake Hand Control Valve |
| 9 - Pressure Protection Valve | 24 - Stop-light Switch |
| 10 - One-way Check Valve | 25 - Combination Double Check Valve |
| 11 - Treadle Valve | 26 - Filler Valve |
| 12 - Ratio Valve | |
| 13 - Quick Release Valve | |
| 14 - Front Service Brake Chamber | |
| 15 - Combination Quick Release Valve | |

Figure 2.1: A general layout of the air brake system in trucks

2.2 THE MECHANICAL SUBSYSTEM

The mechanical subsystem of the S-cam air brake system is illustrated in Fig. 2.2. Compressed air acts on the brake chamber diaphragm providing a mechanical force that is transmitted to the brake pads through the push rod and the S-cam. The force output from the push rod to the brake pads decreases rapidly when its stroke exceeds a certain limit [16]. The stroke of the push rod increases due to the wear of the brake linings and also due to the expansion of the brake drum as a consequence of the heat generated during braking. Automatic slack adjusters are used to compensate for this increase in stroke.

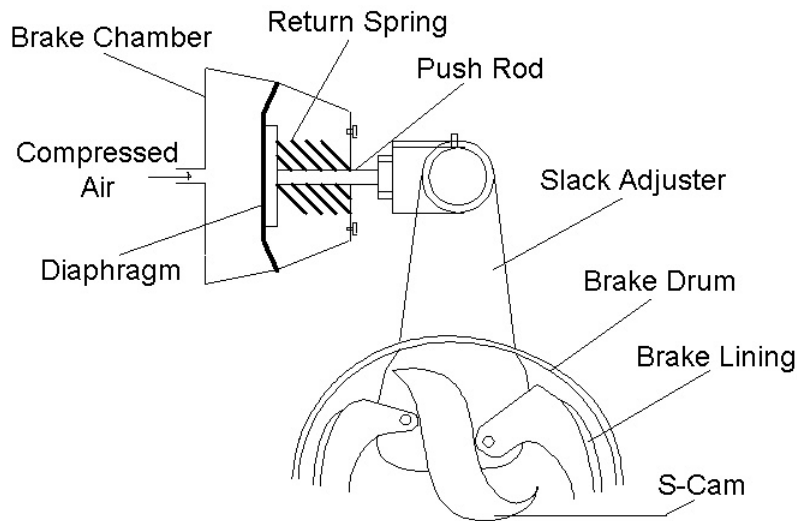


Figure 2.2: The mechanical subsystem of a S-cam air brake system

Drum brakes (see Fig. 2.3) are the most common foundation brakes found in commercial vehicles in the United States, whereas in Europe disc brakes have been slowly replacing drum brakes over the past decade [19]. Disc brakes offer lower sensitivity of the brake torque to the brake pad friction coefficient, better fade resistance and improved brake efficiency when compared to drum brakes. Their main limitation is the absence of “self-energization” [19] (this term refers to the augmentation of the moment due to the actuation force acting on the brake pad by the moment due to the friction force acting on the brake pad) available in drum brakes resulting in the need for higher actuation air pressures when compared to drum brakes.

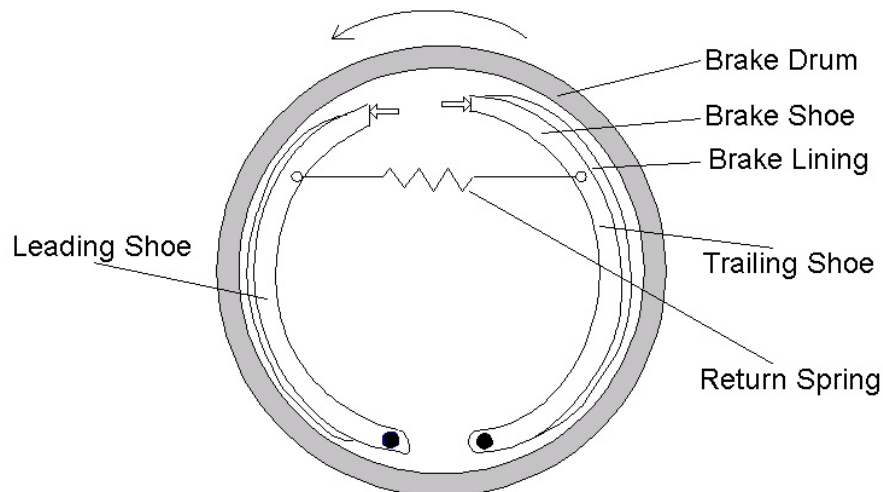


Figure 2.3: A schematic of a drum brake

CHAPTER 3: THE EXPERIMENTAL SETUP

The experimental test bench at Texas A&M University is essentially the front axle of a tractor. Compressed air, supplied by a compressor, is stored in a storage reservoir. A pressure regulator is provided to modulate the pressure of the air being supplied to the treadle valve. Figure 3.1 shows a schematic of the experimental setup. Figure 3.2 and Fig. 3.3 show photographs of the experimental setup. Table (3.1) lists details of the equipment and transducers used in the experimental setup.

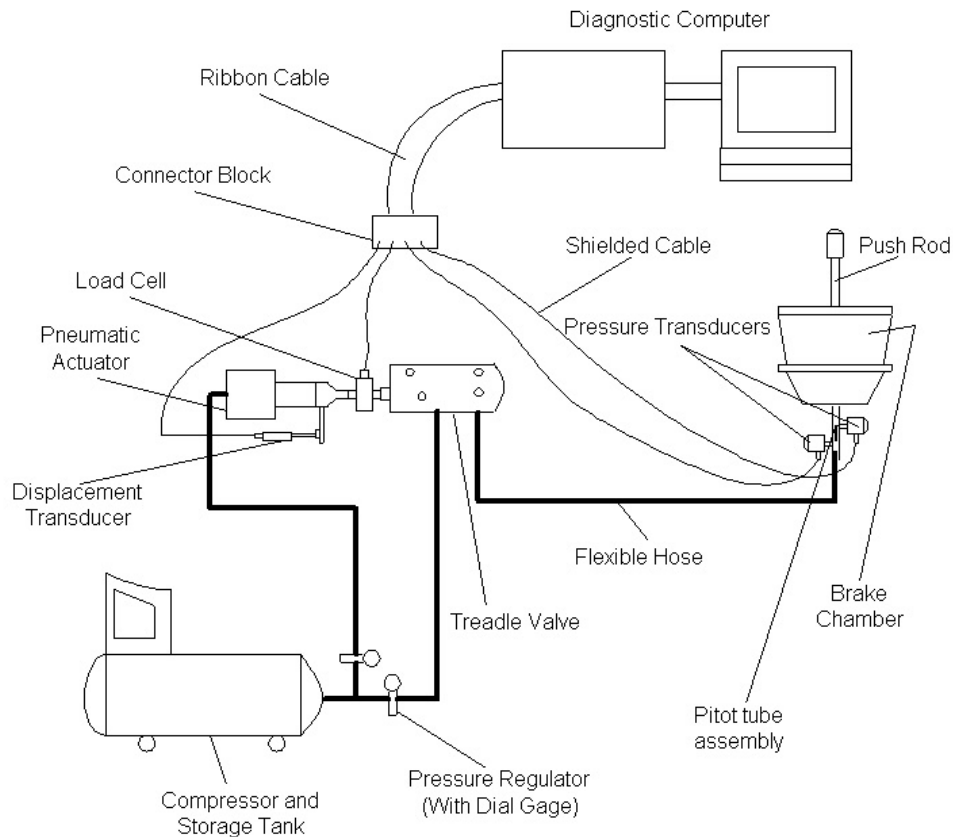


Figure 3.1: A schematic of the experimental setup

The treadle valve used is the E-7 dual circuit valve manufactured by Allied Signals/Bendix (see Fig. 4.1). The primary circuit is actuated by the pedal force and the secondary circuit acts essentially as a relay valve. Under normal operating conditions, air bled off from the primary delivery is used to actuate a relay piston which in turn actuates the secondary circuit. When the primary circuit fails, the secondary circuit is actuated directly by pedal force. When the brake pedal is applied, the primary piston first closes the primary exhaust and then opens the primary inlet valve. This phase is called the “apply phase”. When the delivery pressure increases to a level where it balances the pedal input force, the primary inlet valve is closed with the primary exhaust also remaining closed. This phase is called the “balance or the hold phase”. When the pedal is released, so is the balancing force on the primary piston, which causes the primary

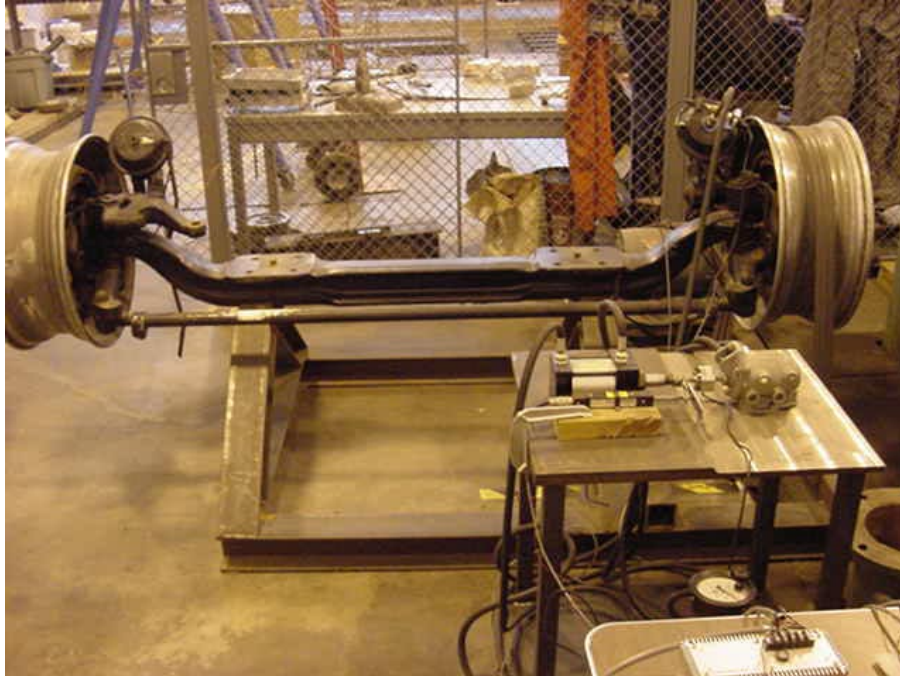


Figure 3.2: A view of the experimental setup



Figure 3.3: Another view of the experimental setup

piston to lift off from the primary exhaust seat and the air in the delivery circuit is exhausted to the atmosphere thereby releasing the brakes. This phase is referred to as the exhaust phase. The secondary circuit functions in a similar manner except for the fact that the relay piston is used to actuate it under normal operating conditions.

The compressed air from the treadle valve is supplied to the brake chamber through brake hoses. A pneumatic actuator is used to apply the treadle valve. The air supply to the pneumatic actuator is provided from the storage tank through a pressure regulator similar to the one used for regulating the supply pressure to the treadle valve. The brake chamber is a “Type-20” brake chamber, i.e., it has a cross-sectional area of 0.0129 m^2 (20 in^2). The stroke of the push rod rotates the S-cam through the automatic slack adjuster. The rotation of the S-cam in turn pushes the brake shoes against the brake drum.

The axial displacement of the treadle valve is measured with a linear potentiometer. The potentiometer has been calibrated and it is found to be linear in the range of interest. A load cell is mounted between the actuating shaft of the pneumatic actuator and the plunger on the brake pedal to measure the pedal force input. A pitot tube assembly was specially fabricated and calibrated in order to infer the Mach numbers of the flow at the entrance of the brake chamber. The pitot tube was mounted at the entrance of the brake chamber and two pressure transducers were used to measure the static and the stagnation pressures. The transducers are interfaced with a connector block through shielded cables. Data is collected through a Data Acquisition (DAQ) board and the connector block is interfaced with the DAQ board via a ribbon cable. An application program written in MATLAB records all the collected data and plots it. A low-pass digital filter [21], with a cut-off frequency of 20 Hz., is used to filter the collected data.

Table 3.1: Details of the equipment and transducers used in the experiment

Title	Manufacturer	Part number	Description
Compressor and storage tank	Campbell Hausfeld		The storage tank has a six gallon capacity.
Pressure regulator	Omega Engineering	PRG501-120	It has a regulation range of 2-120 psig.
Linear potentiometer	Omega Engineering	LP802-75	It has a maximum stroke of 3 " .
Load cell	Omega Engineering	LC203-1K	It has a capacity of 1000 lb.
Pressure transducer	Omega Engineering	PX181-100G5V	It has a range of 0-100 psig.
Power supply	Omega Engineering	PSS-5A	It provides a 5 V d.c. power supply to the linear potentiometer.
Power supply and amplifier	Omega Engineering	DMD-465WB	It provides a 10 V d.c. excitation to the load cell and also amplifies the output from the load cell.
Power supply	Omega Engineering	U24Y101	It provides a 24 V d.c. power supply to the pressure transducer.
Data acquisition board	National Instruments	PCI-1200	It handles a maximum of 4 differential analog inputs.

CHAPTER 4: MODELING THE AIR BRAKE SYSEM

We adopted a lumped parameter approach in modeling the pneumatic subsystem of the air brake system. A model for the pneumatic subsystem of the air brake system must take into consideration the dynamics of the treadle valve and the flow of air in the system. We will now derive the equations of motion of the components of the treadle valve.

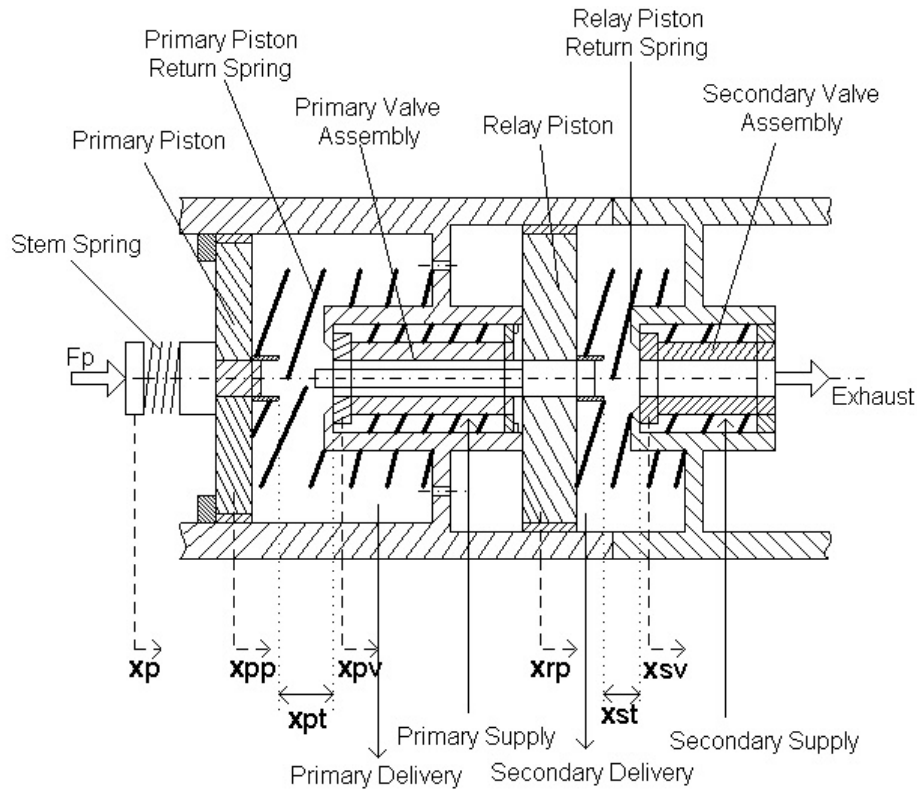


Figure 4.1: A sectional view of the E-7 dual circuit valve

Let F_p denote the force input to the valve plunger. Let x_p denote the axial displacement of the plunger from its initial position. Let x_{pp} and x_{pv} denote the displacement of the primary piston and the primary valve assembly gasket from their initial positions respectively. Let x_{pt} denote the distance traveled by the primary piston before it closes the primary exhaust. Let K_{ss} , K_{pp} and K_{pv} denote the spring constants of the stem spring, the primary piston return spring and the primary valve assembly return spring respectively. Let x_{rp} and x_{sv} denote the displacement of the relay piston and the secondary valve assembly gasket from their initial positions respectively. Let x_{st} denote the distance traveled by the relay piston before it closes the secondary exhaust. Let K_{rp} and K_{sv} denote the spring constants of the relay piston return spring and the secondary valve assembly return spring respectively.

We assume the friction at the sliding surfaces to be negligible. This is reasonable since the sliding surfaces are lubricated with grease. The springs in the treadle valve were tested and found to be linear in the region of their operation. Thus, we can describe the springs by the constitutive equation, $F = Kx$, where F is the net force applied on the spring, x is the deflection of the spring from its initial position and K is the spring constant. The spring constants and the initial pre-loads on the springs were measured and used in the model. Geometric parameters such as areas, initial deflections, etc. were also measured and used in the following equations.

4.1 THE PRIMARY CIRCUIT

We model the primary circuit for its different phases of operation. The equation of motion of the primary piston till it closes the exhaust port can be written as,

$$M_{pp} \left(\frac{d^2 x_{pp}}{dt^2} \right) = F_p - K_{ss} (x_{pp} - x_p) - K_{pp} x_{pp} - F_{kppi} \quad (1)$$

where M_{pp} is the mass of the primary piston and F_{kppi} is the initial pre-load on the primary piston return spring.

The equation of motion of the primary piston during the apply and hold phases can be written as,

$$M_{pp} \left(\frac{d^2 x_{pp}}{dt^2} \right) = F_p - K_{ss} (x_{pp} - x_p) - K_{pp} x_{pp} - F_{kppi} - F_{pp} - F_{reacn}^{p1} - F_{reacn}^{p2} \quad (2)$$

where F_{pp} is the net pressure force acting on the primary piston, F_{reacn}^{p1} is the reaction force applied by the primary valve assembly gasket on the primary piston and F_{reacn}^{p2} is the reaction force applied by the relay piston stem on the primary piston.

The equation of motion of the primary valve assembly gasket during the apply and hold phases can be written as,

$$M_{pv} \left(\frac{d^2 x_{pv}}{dt^2} \right) = F_{reacn}^{p1} - K_{pv} x_{pv} - F_{kpvi} - F_{pv} \quad (3)$$

where M_{pv} is the mass of the primary valve assembly gasket, F_{kpvi} is the initial pre-load on the primary valve assembly return spring and F_{pv} is the net pressure force acting on the primary valve assembly gasket.

Adding Eq. (2) and Eq. (3) and re-arranging the terms results in,

$$\begin{aligned} & M_{pp} \left(\frac{d^2 x_{pp}}{dt^2} \right) + (K_{ss} + K_{pp}) x_{pp} + K_{pv} x_{pv} \\ & = K_{ss} x_p + F_p - F_{kppi} - F_{kpvi} - F_{pp} - F_{pv} - F_{reacn}^{p2} \end{aligned} \quad (4)$$

The three stages of operation of the primary circuit can be described by the following relations:

- Apply Phase

$$x_{pp} > x_{pt} \quad (5)$$

- Hold Phase

$$x_{pp} = x_{pt} \quad (6)$$

- Exhaust Phase

$$x_{pp} < x_{pt} \quad (7)$$

Now, at any instant of time during the apply and hold phases,

$$x_{pv}(t) = x_{pp}(t) - x_{pt} \quad (8)$$

Making use of Eq. (8), we can rewrite Eq. (4) as the following,

$$\begin{aligned} & (M_{pp} + M_{pv}) \left(\frac{d^2 x_{pp}}{dt^2} \right) + (K_{ss} + K_{pp} + K_{pv}) x_{pp} - K_{pv} x_{pt} \\ & = K_{ss} x_p + F_p - F_{kppi} - F_{kpvi} - F_{pp} - F_{pv} - F_{reactn}^{p2} \end{aligned} \quad (9)$$

We note that the three terms $K_{pv} x_{pt}$, F_{kppi} and F_{kpvi} are independent of time and hence combine them as a single constant F_1 given by,

$$F_1 = K_{pv} x_{pt} - F_{kppi} - F_{kpvi} \quad (10)$$

Next, we define the constant K_2 as,

$$K_2 = K_{ss} + K_{pp} + K_{pv} \quad (11)$$

Now, let us look at the term F_{pp} , which is the pressure force acting on the primary piston due to the primary delivery air. Let A_{pp} be the net area of the primary piston exposed to the delivered pressurized air. Assuming the pressure to be uniform over the surface of the primary piston, the term F_{pp} can be written as,

$$F_{pp} = (P_{pd} - P_{atm}) A_{pp} \quad (12)$$

where P_{pd} is the pressure of the primary delivery air at any instant of time and P_{atm} is the atmospheric pressure (all the pressure terms used here represent absolute pressures).

Next, let us consider the term F_{pv} , which is the net pressure force acting on the primary valve assembly gasket. Let A_{pv1} and A_{pv} be the net cross-sectional area of the primary valve assembly gasket exposed to the pressurized air at the supply and the delivery respectively. Under the same assumptions as above and also assuming the gasket to be sufficiently rigid (which is reasonable since the gasket is enclosed by a metal ring), we can write the expression for F_{pv} as,

$$F_{pv} = P_{ps}A_{pv1} - P_{pd}A_{pv} \quad (13)$$

where P_{ps} is the supply air pressure to the primary circuit.

Using Eq. (10) to Eq. (13), Eq. (9) can be now written as,

$$\begin{aligned} (M_{pp} + M_{pv}) \left(\frac{d^2 x_{pp}}{dt^2} \right) + K_2 x_{pp} = K_{ss} x_p + F_p + F_1 \\ - P_{pd}(A_{pp} - A_{pv}) - P_{ps}A_{pv1} - F_{reacn}^{p2} + P_{atm}A_{pp} \end{aligned} \quad (14)$$

Equation (14) represents the dynamics of the primary circuit during the apply and hold phases. We now neglect the inertia of the primary piston and the primary valve assembly gasket compared to the other forces. Let us consider the primary piston to support this approximation. The mass of the primary piston was found out to be around 0.16 kg and the magnitude of the spring and pressure forces was found to be in the order of 10^2 N. Thus, the acceleration required for the inertial forces to be comparable with the spring force and the pressure force terms has to be in the order of $10^2 - 10^3$ m/s², which is not possible in this case. With this simplification, the above equation reduces to the following,

$$K_2 x_{pp} = K_{ss} x_p + F_p + F_1 - P_{pd}(A_{pp} - A_{pv}) - P_{ps}A_{pv1} - F_{reacn}^{p2} + P_{atm}A_{pp} \quad (15)$$

This equation is used with Eq. (64), which will be derived in section (4.3), to obtain the response of the primary circuit to various pedal inputs. The term F_{reacn}^{p2} is obtained from Eq. (20), which will be derived in the following subsection. It should be noted that this term will be present in the above equation only till the primary piston and the primary valve assembly are in contact with the relay piston. At some point during the apply phase, this contact would be broken and then this term would be set to zero.

Next, we look at the equation of motion of the primary piston during the exhaust phase. During the exhaust phase, the primary piston would break off from the primary valve assembly gasket and thus uncovers the exhaust port. We define x_{ppe} and x_{pe} as the displacement of the primary piston and the treadle valve plunger from their equilibrium positions at the start of the exhaust phase respectively. The equation of motion of the primary piston in this case can be written as,

$$M_{pp} \left(\frac{d^2 x_{ppe}}{dt^2} \right) = F_{pp} - F_p - K_{ss}(x_{ppe} - x_{pe}) - K_{pp}x_{ppe} + F_{kppie} \quad (16)$$

where F_{kppie} is the pre-load on the primary piston return spring at the start of the exhaust phase.

Neglecting the inertia of the primary piston and using Eq. (12), the above equation can be simplified as,

$$L_2 x_{ppe} = K_{ss} x_{pe} - F_p + L_1 + P_{pd}A_{pp} - P_{atm}A_{pp} \quad (17)$$

where we define L_1 and L_2 in the following way:

$$L_1 = F_{kppie} \quad (18)$$

$$L_2 = K_{ss} + K_{pp} \quad (19)$$

Equation (17) governs the motion of the primary piston during the exhaust phase. This equation is used along with the equation governing the fluid flow developed in section (4.3) to obtain the pressure transients in the primary circuit during the exhaust phase.

4.2 THE SECONDARY CIRCUIT

We now model the secondary circuit of the treadle valve for its various phases of operation. The equation of motion of the relay piston till it closes the exhaust port is given by,

$$M_{rp} \left(\frac{d^2 x_{rp}}{dt^2} \right) = F_{reacn}^{p2} + F_{rpd} - K_{rp} x_{rp} - F_{krpi} - P_{atm} A'_{rp} \quad (20)$$

where M_{rp} is the mass of the relay piston, F_{reacn}^{p2} is the net mechanical force transmitted by the primary circuit to the relay piston, F_{rpd} is the pressure force acting on the relay piston due to the air bled from the primary delivery, F_{krpi} is the initial pre-load on the relay piston return spring and A'_{rp} is the net area of the relay piston exposed to the secondary delivery air.

During the apply and hold phases of the secondary circuit, the equation of motion for the relay piston is,

$$M_{rp} \left(\frac{d^2 x_{rp}}{dt^2} \right) = F_{reacn}^{p2} + F_{rpd} - K_{rp} x_{rp} - F_{krpi} - F_{sp} - F_{reacn}^s \quad (21)$$

where F_{sp} is the net pressure force acting on the relay piston as a result of the increasing secondary delivery pressure and F_{reacn}^s is the reaction force exerted by the secondary valve assembly gasket on the relay piston.

The equation of motion for the secondary valve assembly gasket during the apply and hold phases can be written as,

$$M_{sv} \left(\frac{d^2 x_{sv}}{dt^2} \right) = F_{reacn}^s - K_{sv} x_{sv} - F_{ksvi} - F_{sv} \quad (22)$$

where M_{sv} is the mass of the secondary valve assembly gasket, F_{ksvi} is the initial pre-load on the secondary valve assembly return spring and F_{sv} is the net pressure force acting on the secondary valve assembly gasket.

Adding Eq. (21) and Eq. (22), we obtain,

$$M_{rp} \left(\frac{d^2 x_{rp}}{dt^2} \right) + M_{sv} \left(\frac{d^2 x_{sv}}{dt^2} \right) = F_{reacn}^{p2} + F_{rpd} - K_{rp} x_{rp} - F_{krpi} - F_{sp} - K_{sv} x_{sv} - F_{ksvi} - F_{sv} \quad (23)$$

The three stages of operation of the secondary circuit can be described by the following relations:

- Apply Phase

$$x_{rp} > x_{st} \quad (24)$$

- Hold Phase

$$x_{rp} = x_{st} \quad (25)$$

- Exhaust Phase

$$x_{rp} < x_{st} \quad (26)$$

Next, we note that at any instant of time during the apply and hold phases,

$$x_{sv}(t) = x_{rp}(t) - x_{st} \quad (27)$$

Using Eq. (27), Eq. (23) can be rewritten as,

$$\begin{aligned} (M_{rp} + M_{sv}) \left(\frac{d^2 x_{rp}}{dt^2} \right) + (K_{rp} + K_{sv}) x_{rp} - K_{sv} x_{st} \\ = F_{reacn}^{p2} + F_{rpd} - F_{sp} - F_{sv} - F_{krpi} - F_{ksvi} \end{aligned} \quad (28)$$

We note that the three terms $K_{sv} x_{st}$, F_{krpi} and F_{ksvi} are independent of time and hence combine them as a single constant F_3 given by,

$$F_3 = K_{sv} x_{st} - F_{krpi} - F_{ksvi} \quad (29)$$

Next, we define the constant K_4 as,

$$K_4 = K_{rp} + K_{sv} \quad (30)$$

Next, the term F_{rpd} can be expressed as,

$$F_{rpd} = P_{pd} A_{rp} \quad (31)$$

where P_{pd} is the primary delivery air pressure and A_{rp} is the area of the relay piston exposed to the primary delivery air.

Now, the net pressure force, F_{sp} , acting on the relay piston due to the secondary delivery air can be written as,

$$F_{sp} = P_{sd} A'_{rp} \quad (32)$$

where P_{sd} is the secondary delivery air pressure.

Next, the net pressure force, F_{sv} , acting on the secondary valve gasket can be expressed as,

$$F_{sv} = (P_{ss} - P_{sd}) A_{sv} \quad (33)$$

where P_{ss} is the secondary supply air pressure and A_{sv} is the area of the gasket exposed to the pressurized air.

Using Eq. (29) to Eq. (33), Eq. (28) can be rewritten as,

$$\begin{aligned} (M_{rp} + M_{sv}) \left(\frac{d^2 x_{rp}}{dt^2} \right) + K_4 x_{rp} = F_{reacn}^{p2} + P_{pd} A_{rp} \\ - P_{sd} (A'_{rp} - A_{sv}) - P_{ss} A_{sv} + F_3 \end{aligned} \quad (34)$$

Equation (34) represents the dynamics of the secondary circuit during the apply and hold phases. Next, we neglect the inertia of the relay piston and the secondary valve assembly gasket compared to the other forces. Then, the above equation reduces to,

$$K_4 x_{rp} = F_{reacn}^{p2} + P_{pd} A_{rp} - P_{sd} (A'_{rp} - A_{sv}) - P_{ss} A_{sv} + F_3 \quad (35)$$

This equation is used with Eq. (64) to obtain the response of the secondary circuit to various pedal inputs.

Next, we look at the equation of motion of the relay piston during the exhaust phase. During the exhaust phase, the relay piston uncovers the secondary exhaust port. We define x_{rpe} as the displacement of the relay piston from its equilibrium position at the start of the exhaust phase. The equation of motion of the relay piston in this case can be written as,

$$M_{rp} \left(\frac{d^2 x_{rpe}}{dt^2} \right) = F_{sp} + F_{krpie} - K_{rp} x_{rpe} - F_{reacn}^{p2} - F_{rpd} \quad (36)$$

where F_{krpie} is the load on the relay piston return spring at the start of the exhaust phase. Neglecting the inertia of the relay piston and using Eq. (31) and Eq. (32), the above equation is simplified as,

$$K_{rp} x_{rpe} = P_{sd} A'_{rp} + F_{krpie} - P_{pd} A_{rp} - F_{reacn}^{p2} \quad (37)$$

Equation (37) governs the motion of the relay piston during the exhaust phase. It is used along with the equation governing the fluid flow developed in section (4.3) to obtain the pressure transients in the secondary circuit during the exhaust phase.

4.3 MODELING THE FLUID FLOW

We idealize the treadle valve as a nozzle. For the flow through a restriction, if the ratio of the cross-sectional area of the upstream section to the cross-sectional area of the restriction is 4.4 or higher, the approach velocity to this restriction can be neglected and the upstream properties (such as pressure, enthalpy, temperature, etc.) can be taken to be the upstream total or stagnation properties [22]. In this application, the minimum ratio of the cross-sectional area of the supply chamber of the valve to the cross-sectional area of the valve opening (the restriction in our case) was found out to be around 15.4. Also, the cross-sectional area of the valve opening decreases monotonically to a minimum value. Hence, we can consider the valve opening as a nozzle and take the properties in the supply chamber of the valve as the stagnation properties at the inlet section of the nozzle. We assume the flow through this idealized valve to be one-dimensional and isentropic. Further, we assume the fluid properties to be uniform at all sections in the nozzle. We assume air to behave like an ideal gas. Figure 4.2 shows the simplified pneumatic subsystem under the above assumptions.

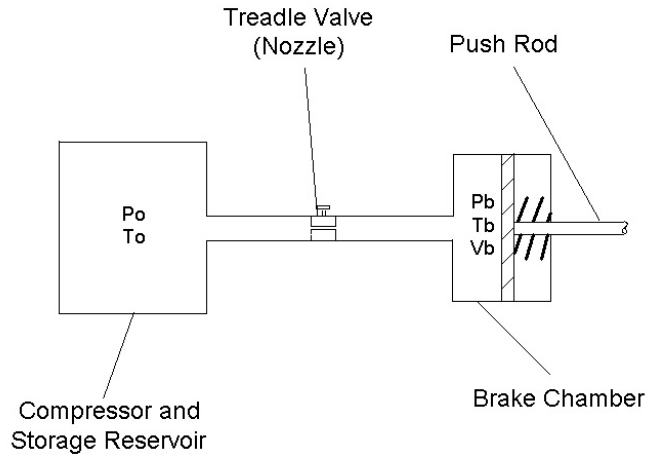


Figure 4.2: The simplified pneumatic subsystem

The energy equation for isentropic flow of air through the nozzle under the above assumptions can be written as [23],

$$h + \frac{1}{2}u^2 = h_o \quad (38)$$

where h_o is the specific stagnation enthalpy at the entrance section of the nozzle, h is the specific enthalpy at the exit section of the nozzle and u is the velocity of air at the exit section of the nozzle.

Since air is considered to be an ideal gas, its specific enthalpy at any point in the flow region can be written as,

$$h = c_p T \quad (39)$$

where c_p is the specific heat of air at constant pressure (assumed to be a constant) and T is the local temperature of the air at that point. Then, Eq. (38) can be rewritten as,

$$c_p T + \frac{1}{2}u^2 = c_p T_o \quad (40)$$

where T_o is the temperature of the compressed air in the storage reservoir.

We have made the assumption that air behaves like an ideal gas. For an ideal gas, the local pressure is a function only of its local density, i.e.,

$$P = P(\rho) \quad (41)$$

where P is the local pressure and ρ is the local density of air.

We use the following ‘‘Ideal Gas Law’’ in the equations below:

$$P(\rho) = \rho RT \quad (42)$$

where R is the gas constant for air and T is the local temperature.

For isentropic flow of an ideal gas, the pressure, density and temperature are related by,

$$\frac{P}{\rho^\gamma} = \text{constant} \quad (43)$$

$$\left(\frac{P^{(\frac{\gamma-1}{\gamma})}}{T} \right) = \text{constant} \quad (44)$$

where γ is the ratio of the specific heats. We assume that this ratio is a constant.

$$\gamma = \frac{c_p}{c_v} \quad (45)$$

where c_v is the specific heat of air at constant volume.

For an ideal gas, the two specific heats are related by,

$$c_p - c_v = R \quad (46)$$

Thus, from Eq. (45) and Eq. (46),

$$\begin{aligned} c_p &= \left(\frac{\gamma}{\gamma-1} \right) R \\ c_v &= \left(\frac{1}{\gamma-1} \right) R \end{aligned} \quad (47)$$

Using Eq. (42) to Eq. (47), Eq. (40) can be solved for the velocity u as,

$$u = \left[\left(\frac{2\gamma}{\gamma-1} \right) \frac{P_o}{\rho_o} \left[1 - \left(\frac{P}{P_o} \right)^{\left(\frac{\gamma-1}{\gamma} \right)} \right] \right]^{\frac{1}{2}} \quad (48)$$

where P_o and ρ_o are the pressure and density of air in the storage reservoir respectively.

Next, we choose the brake chamber and the air hose as the control volume under consideration. We assume all fluid properties in the control volume to be uniform at any instant of time. We assume frictional losses in the hose to be negligible. The Mach number of the flow in the hose was inferred at the entrance of the brake chamber from the measurements of the static and stagnation pressures using the following formula [23]:

$$M = \left(\left(\frac{2}{\gamma-1} \right) \left(\left(\frac{P_s}{P} \right)^{\frac{\gamma-1}{\gamma}} - 1 \right) \right)^{\frac{1}{2}} \quad (49)$$

where M is the local Mach number and P_s is the local stagnation pressure. For various test runs, the value of the Mach number was found not to exceed 0.2. Hence, we can neglect the effects of compressibility of air for the flow through the hose [24].

Applying mass balance to the control volume (see Fig. 4.3), we obtain,

$$\dot{m}_b = \rho u A_p \quad (50)$$

where \dot{m}_b is the time rate of change of the mass of air in the control volume, ρ is the density of air inside the control volume at any instant of time, u is the velocity of air at the exit section of the nozzle. This is the velocity of air entering the control volume and A_p is the cross-sectional area of the valve opening.

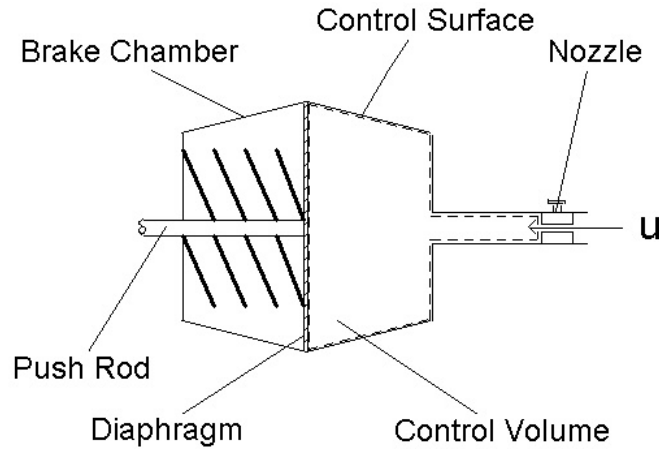


Figure 4.3: The brake chamber as the control volume

The term A_p is given by the following expression,

$$A_p = \begin{cases} 2\pi r_{pv} x_{pv} & \text{during the apply phase} \\ 2\pi r_{pp} x_{ppe} & \text{during the exhaust phase} \end{cases} \quad (51)$$

where r_{pv} is the external radius of the primary valve assembly inlet section and r_{pp} is the external radius of the primary piston exhaust seat.

Next, let us consider the mass of air inside the control volume at any instant of time, m_b . Since we treat air as an ideal gas,

$$m_b = \frac{P_b V_b}{RT_b} \quad (52)$$

where P_b is the local pressure inside the control volume, V_b is the volume of the control volume and T_b is the local temperature inside the control volume at that instant of time.

Differentiating both sides of the above equation with respect to time, we obtain,

$$\dot{m}_b = \frac{\dot{P}_b V_b}{RT_b} + \frac{P_b \dot{V}_b}{RT_b} - \left(\frac{P_b V_b}{RT_b^2} \right) \dot{T}_b \quad (53)$$

Using Eq. (44), Eq. (53) can be simplified as,

$$\dot{m}_b = \left(\frac{1}{\gamma} \right) \frac{\dot{P}_b V_b}{RT_b} + \frac{P_b \dot{V}_b}{RT_b} \quad (54)$$

Let us now consider the variation of the brake chamber volume as a function of time during the brake application. At the start of the application, the brake chamber diaphragm starts to move only after the required “push-out” pressure is reached [18]. This initial increase in pressure is utilized in overcoming the pre-loads of the brake chamber return spring and the return spring in the brake drum. As soon as the push-out pressure is reached, the brake chamber volume starts to increase and as a result, the time rate of growth of the brake chamber pressure decreases. The brake chamber volume reaches its maximum value when the brake pads contact the drum. After this, the time rate of pressure growth starts to increase and the subsequent growth of the brake chamber pressure is utilized in increasing the brake force. These variations are taken into account in this model by varying the expression for the brake chamber volume depending on the phase of operation of the brake chamber diaphragm. The volume of air inside the control volume at any instant of time can be written as,

$$V_b = \begin{cases} V_{o1} & \text{if } P_b < P_t \\ V_{o1} + A_b x_b & \text{if } 0 \leq x_b < x_{bmax} \\ V_{o2} & \text{if } x_b = x_{bmax} \end{cases} \quad (55)$$

where V_{o1} is the initial volume of air in the control volume before the application of the brake, V_{o2} is the maximum volume of air in the control volume, A_b is the cross-sectional area of the brake chamber, x_b is the stroke of the brake chamber diaphragm, i.e., the stroke of the push rod, x_{bmax} is the maximum stroke of the push rod and P_t is the “push-out” pressure.

Using the above equation, Eq. (54) can be written as,

$$\dot{m}_b = \begin{cases} \left(\frac{V_{o1}}{\gamma RT_b} \right) \dot{P}_b & \text{if } P_b < P_t \\ \left(\frac{V_b}{\gamma RT_b} \right) \dot{P}_b + \left(\frac{P_b A_b}{RT_b} \right) \dot{x}_b & \text{if } 0 \leq x_b < x_{bmax} \\ \left(\frac{V_{o2}}{\gamma RT_b} \right) \dot{P}_b & \text{if } x_b = x_{bmax} \end{cases} \quad (56)$$

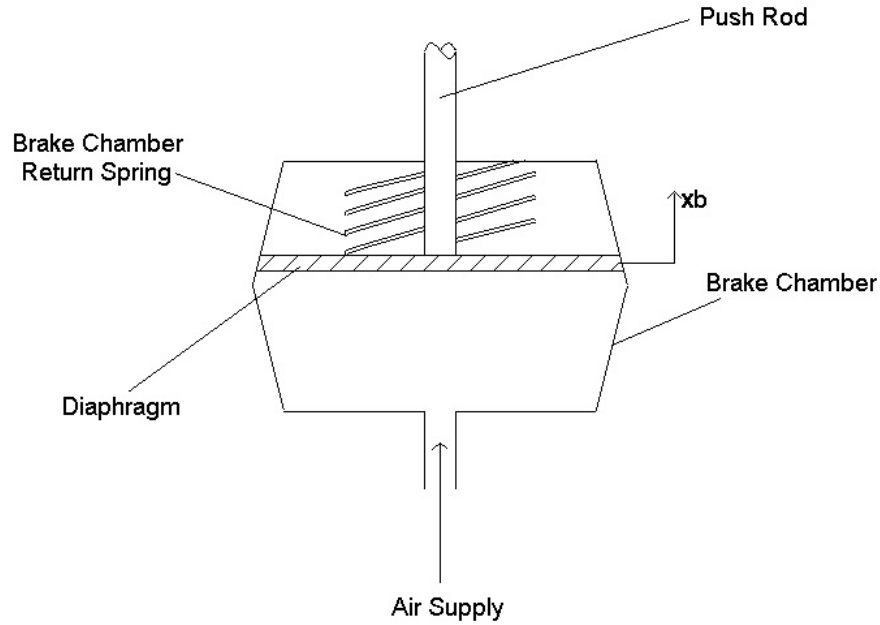


Figure 4.4: A sectional view of the brake chamber

Let us now consider the dynamics of the brake chamber (refer to Fig. 4.4). The equation of motion of the brake chamber diaphragm can be written as (we neglect any friction in the brake chamber),

$$M_b \left(\frac{d^2 x_b}{dt^2} \right) + K_b x_b = (P_b - P_{atm}) A_b - F_{kbi} \quad (57)$$

where M_b is the mass of the brake chamber diaphragm, K_b is the spring constant of the brake chamber return spring and F_{kbi} is the pre-load on the brake chamber diaphragm return spring.

We make an additional simplification by neglecting the inertia of the brake chamber diaphragm. Thus, the above equation reduces to,

$$x_b = \frac{(P_b - P_{atm})A_b - F_{kbi}}{K_b} \quad (58)$$

Using Eq. (58) in Eq. (56), and simplifying yields,

$$\dot{m}_b = \begin{cases} \left(\frac{V_{o1}}{\gamma RT_b} \right) \dot{P}_b & \text{if } P_b < P_t \\ \left(\frac{V_b}{\gamma RT_b} + \frac{P_b A_b^2}{RT_b K_b} \right) \dot{P}_b & \text{if } 0 \leq x_b < x_{bmax} \\ \left(\frac{V_{o2}}{\gamma RT_b} \right) \dot{P}_b & \text{if } x_b = x_{bmax} \end{cases} \quad (59)$$

Equation (48) gave us a relationship to calculate the velocity of air at the exit section of the nozzle. We modify this equation with a discharge coefficient C_D in order to compensate for the losses during the flow. Due to the complexity involved in calibrating the valve to determine the value of the discharge coefficient, we assumed a value of 0.82 for C_D as recommended in [22]. Also, we modify the equation so that the direction of the flow is incorporated.

$$u = C_D \left(\frac{2\gamma}{\gamma-1} \right) \frac{P_o}{\rho_o} \left[\left[1 - \left(\frac{P_b}{P_o} \right)^{\left(\frac{\gamma-1}{\gamma} \right)} \right] \right]^{\frac{1}{2}} \text{sgn}(P_o - P_b) \quad (60)$$

The signum function used in the above equation is defined as,

$$\text{sgn}(P_o - P_b) := \frac{P_o - P_b}{|P_o - P_b|} \quad (61)$$

Thus, the signum function indicates the direction of flow depending on the pressure difference. During the apply and the hold phases, P_o is the supply pressure and during the exhaust phase, P_o is the atmospheric pressure.

Now using Eq. (42) and Eq. (60), Eq. (50) can be re-written as,

$$\dot{m}_b = \left(\left(\frac{2\gamma}{\gamma-1} \right) \frac{P_o}{\rho_o} \left[\left[1 - \left(\frac{P_b}{P_o} \right)^{\left(\frac{\gamma-1}{\gamma} \right)} \right] \right] \right)^{\frac{1}{2}} \frac{P_b A_p C_D}{RT_b} \text{sgn}(P_o - P_b) \quad (62)$$

When the pressure ratio is less than the critical value, choked flow conditions are assumed and the mass flow rate is maximum through the nozzle under this condition. The critical pressure ratio is given by,

$$\left(\frac{P_b}{P_o}\right)_{cr} = \left(\frac{2}{\gamma+1}\right)^{\left(\frac{\gamma}{\gamma-1}\right)} \quad (63)$$

Now, comparing Eq. (59) and Eq. (62) and simplifying using Eq. (42) and Eq. (44), we obtain the governing equation for the pressure transients in the brake chamber for the various phases of the motion of the brake chamber diaphragm.

$$\left(\left(\frac{2\gamma}{\gamma-1}\right)\frac{1}{RT_o}\left[\left(\frac{P_b}{P_o}\right)^{\left(\frac{2}{\gamma}\right)} - \left(\frac{P_b}{P_o}\right)^{\left(\frac{\gamma+1}{\gamma}\right)}\right]\right)^{\frac{1}{2}} A_p C_D P_o \text{sgn}(P_o - P_b) = \begin{cases} \left(\frac{V_{o1} P_o^{\left(\frac{\gamma-1}{\gamma}\right)}}{\gamma RT_o P_b^{\left(\frac{\gamma-1}{\gamma}\right)}}\right) \dot{P}_b \text{ if } P_b < P_t \\ \left(\frac{V_b P_o^{\left(\frac{\gamma-1}{\gamma}\right)}}{\gamma RT_o P_b^{\left(\frac{\gamma-1}{\gamma}\right)}} + \frac{P_b^{\frac{1}{\gamma}} A_b^2 P_o^{\left(\frac{\gamma-1}{\gamma}\right)}}{RT_o K_b}\right) \dot{P}_b \text{ if } 0 \leq x_b < x_{bmax} \\ \left(\frac{V_{o2} P_o^{\left(\frac{\gamma-1}{\gamma}\right)}}{\gamma RT_o P_b^{\left(\frac{\gamma-1}{\gamma}\right)}}\right) \dot{P}_b \text{ if } x_b = x_{bmax} \end{cases} \quad (64)$$

This is the governing equation for the pressure transients in the brake chamber during the apply phase with the term P_o being the supply pressure. The coefficients of the above equation are now functions of P_b and A_p and this equation has to be solved with the initial condition that at the start of the apply phase, $P_b = P_{atm}$. At each time step during the apply phase, the value of the pressure obtained from this equation is used to determine the stage of operation of the two circuits through Eq. (15) and Eq. (35). Equation (51) and Eq. (55) are used to evaluate the terms A_p and V_b in the above equation at any instant of time. At any instant of time, if the pressure ratio is less than the critical value, then the critical pressure ratio is used while solving Eq. (64). When the pressure ratio becomes greater than the critical value, the actual pressure ratio is used.

For the exhaust phase, the term P_o is taken to be the atmospheric pressure and the term T_o is taken to be the atmospheric temperature. The governing differential equation is solved with the initial condition that at the start of the exhaust phase, the pressure in the brake chamber is the steady state pressure at the end of the apply phase. The brake chamber volume is the maximum at the start of the exhaust phase and decreases as the exhaust phase progresses according to the following equation,

$$V_b = \begin{cases} V_{o2} \text{ if } x_{be} = 0 \\ V_{o2} - A_b x_{be} \text{ if } 0 \leq x_{be} < x_{bmax} \\ V_{o1} \text{ if } x_{be} = x_{bmax} \end{cases} \quad (65)$$

where x_{be} is the displacement of the brake chamber diaphragm from its equilibrium position at the start of the exhaust phase.

CHAPTER 5: CORROBORATION OF THE MODEL

In this section, we corroborate the model for the operation of the primary circuit. Equation (64) was solved numerically using the fourth order Runge-Kutta method. A time step of 0.0001 seconds was used. Experiments were conducted at various supply pressures and the brake was applied using the actuator. Equation (15) was used to determine the start and the termination of the simulation. The simulation for the apply phase was started when the value of x_{pv} became greater than zero which corresponds to the opening of the treadle valve. Two conditions determine the termination of the apply phase - the value of x_{pv} becoming less than or equal to zero (which corresponds to the closure of the valve) and the brake chamber pressure becoming equal to the supply pressure. The simulation ends when either one of these two conditions is satisfied. The inputs to the simulation are the pedal force F_p and the plunger displacement x_p . The parameters used in the simulation were measured and the values of the parameters are tabulated in Table (5.1). The results are shown in Fig. 5.1 to Fig. 5.3.

Table 5.1: Values of the parameters used in the simulation

Parameter	Value	Parameter	Value
A_{pv}	0.0002356 m^2	A_{pv1}	0.0004184 m^2
A_{pp}	0.002357 m^2	A_b	0.0129 m^2
A_{rp}	0.001985 m^2	A'_{rp}	0.003141 m^2
K_b	1167.454 N/m	K_{ss}	2556.724 N/m
F_1	-193.832 N	K_2	8178.716 N/m
L_1	68.944 N	L_2	6418.078 N/m
x_{pt}	0.00127 m	P_{atm}	101.356 KPa
r_{pv}	0.01283 m	r_{pp}	0.01232 m
γ	1.4	V_{o1}	0.0001639 m^3
x_{bmax}	0.0254 m	F_{kbi}	355.84 N
R	287 $J/(kgK)$	T_o	298 K
C_D	0.82		

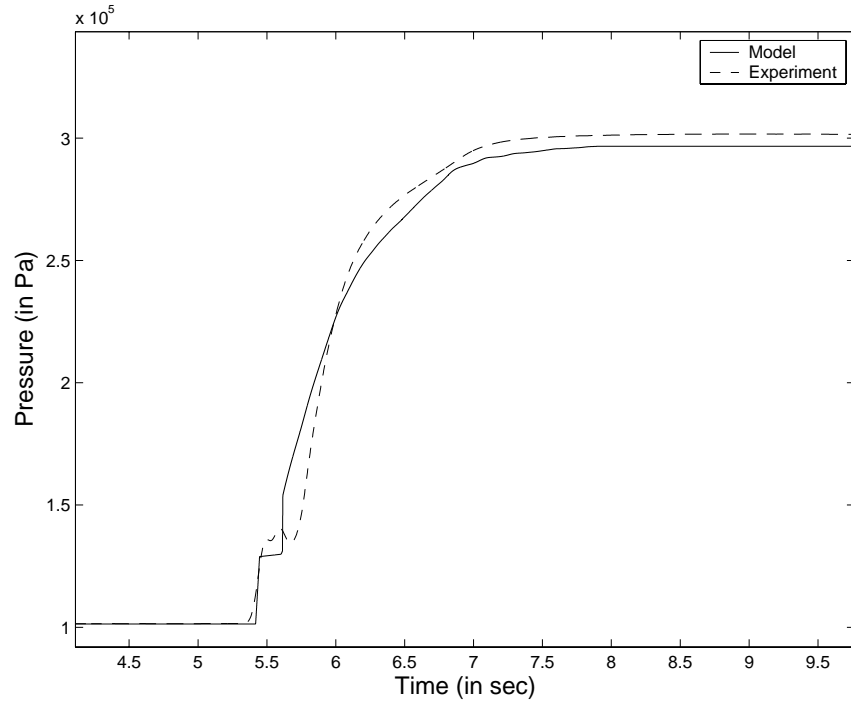


Figure 5.1: Pressure transients at 515 KPa (60 psig) supply pressure – apply phase

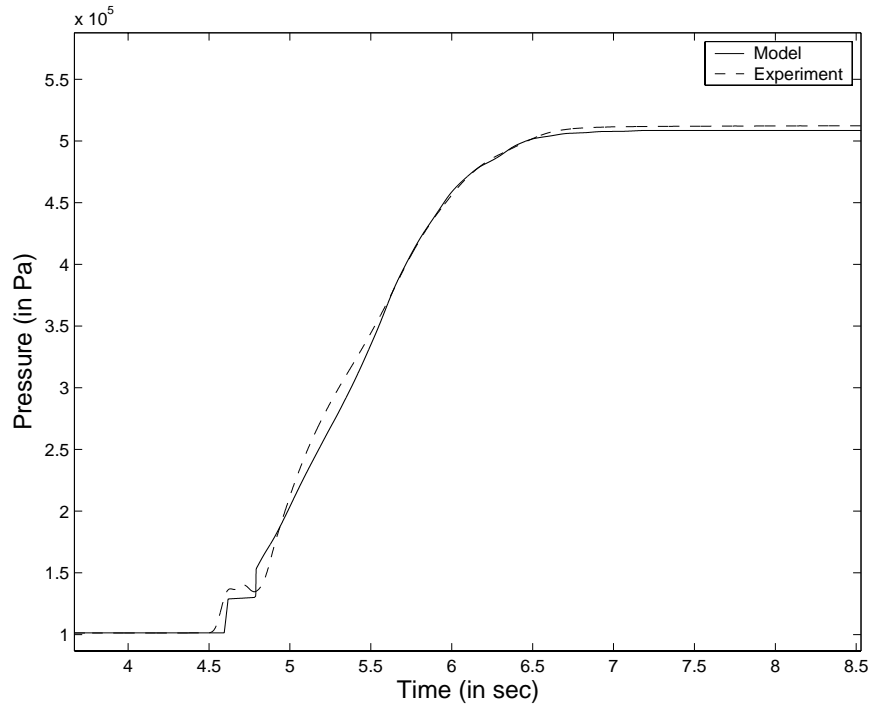


Figure 5.2: Pressure transients at 653 KPa (80 psig) supply pressure - apply phase

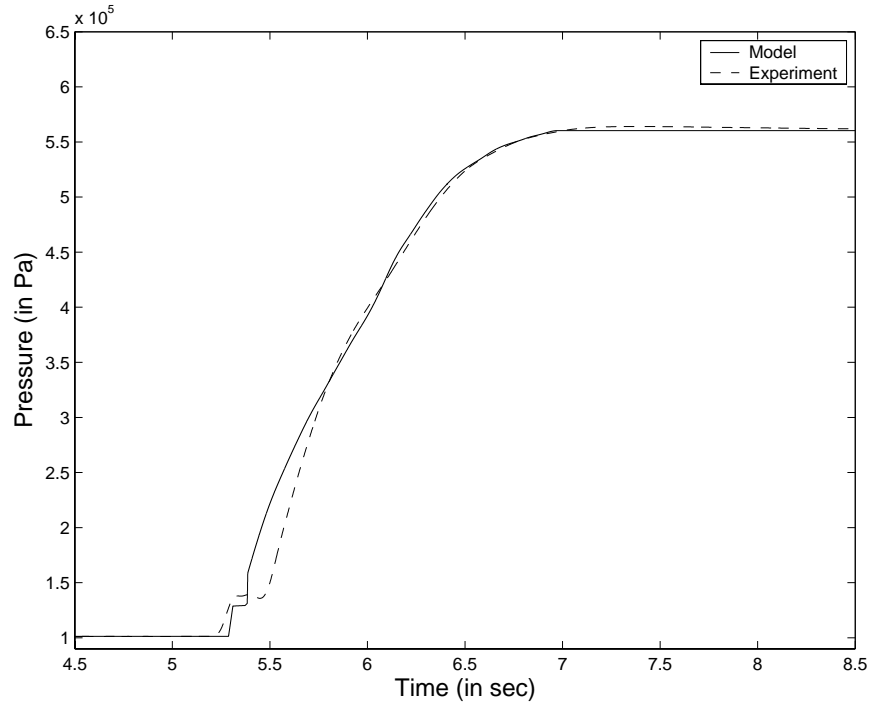


Figure 5.3: Pressure transients at 722 KPa (90 psig) supply pressure - apply phase

We can observe from Fig. 5.1 to Fig. 5.3 that the model is able to predict the start and the end of the brake application for all the cases. The steady state value of the brake chamber pressure is also predicted accurately. We can also observe that the model is able to follow the initial behavior of the pressure growth curve since we divided the operation of the brake chamber into three different phases.

We also performed tests for a complete cycle of brake application. The model was used to simulate both the apply and the exhaust phases for such applications. The results are shown in Fig. 5.4 to Fig. 5.6. Finally, a test run was performed where the apply and the exhaust phases were periodically repeated. Results from such a test run are shown in Fig. 5.7.

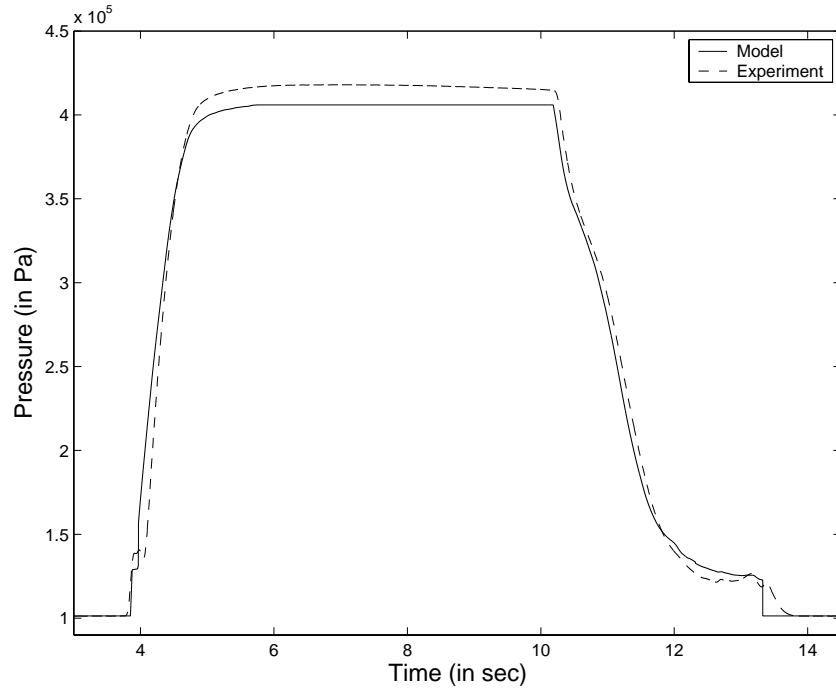


Figure 5.4: Pressure transients at 584 KPa (70 psig) supply pressure - apply and exhaust phases

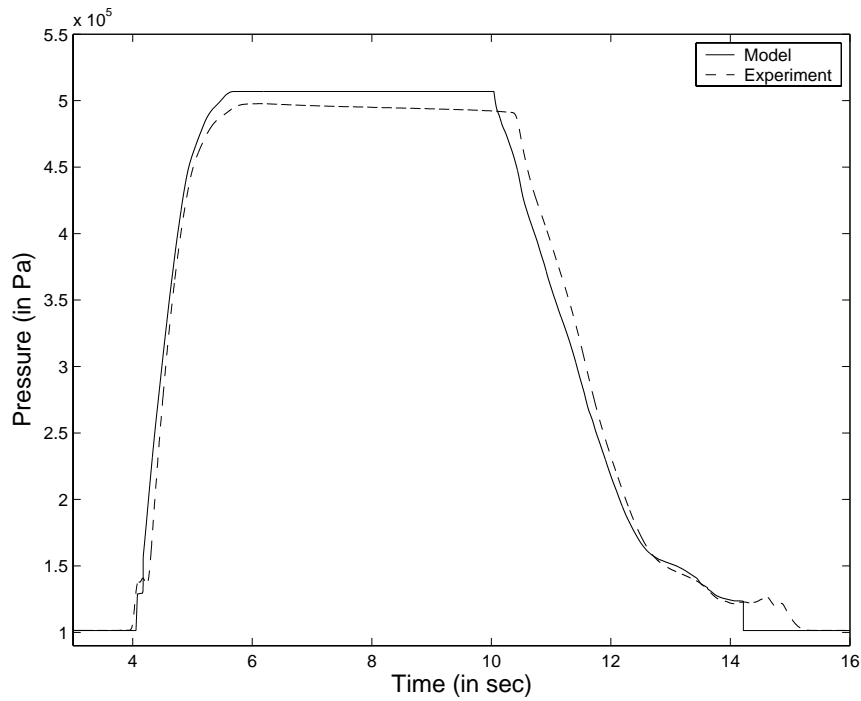


Figure 5.5: Pressure transients at 653 KPa (80 psig) supply pressure - apply and exhaust phases

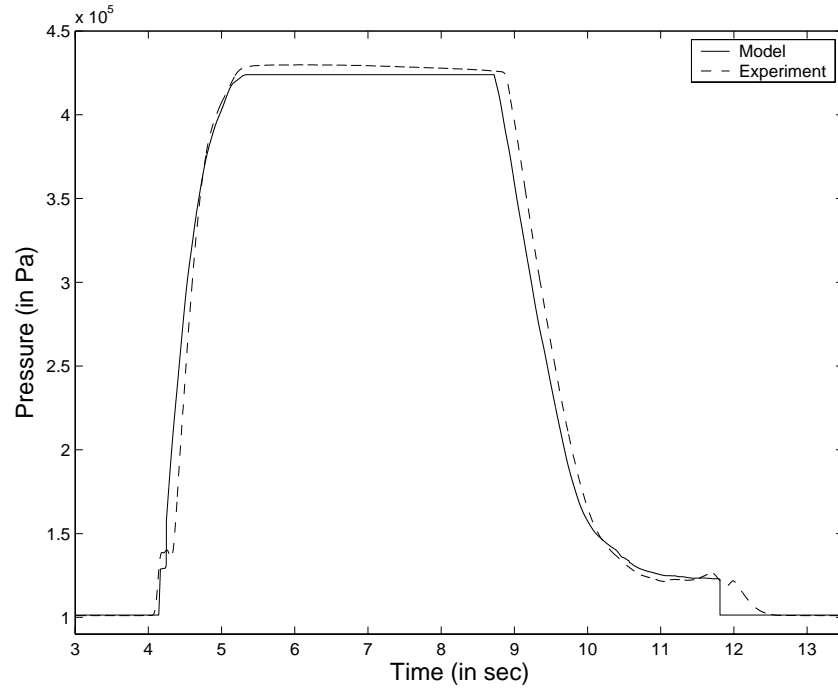


Figure 5.6: Pressure transients at 722 KPa (90 psig) supply pressure - apply and exhaust phases

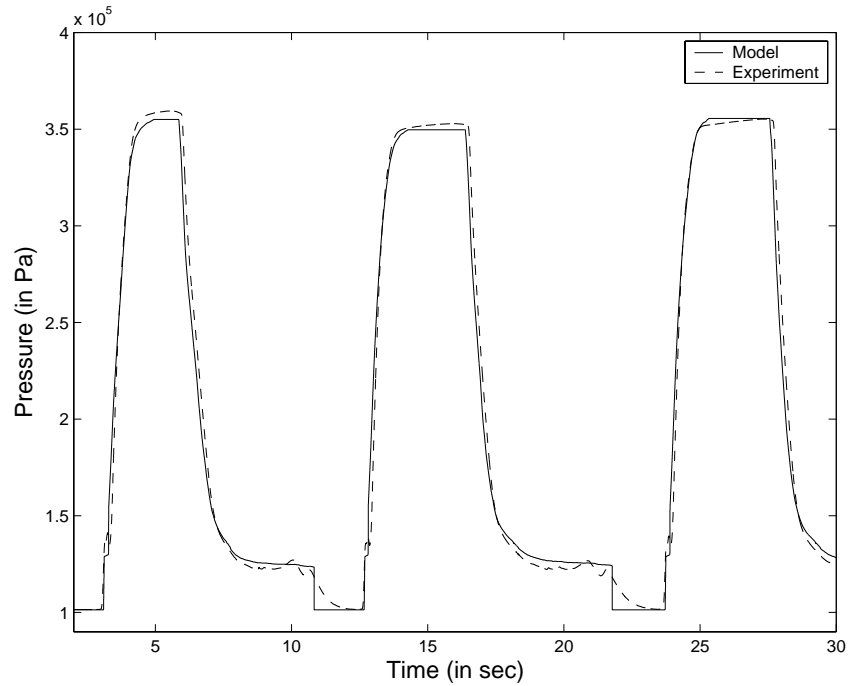


Figure 5.7: Pressure transients at 584 KPa (70 psig) supply pressure - periodic application

CHAPTER 6: CONCLUDING REMARKS

From the above figures, it can be seen that the model was able to predict the beginning and the end of each brake application accurately. The steady state values are also accurately predicted by the model in all the cases. We observe that the model responded well to various supply pressures. The model also predicted the start and the termination of the exhaust phase accurately as was evident from Fig. 5.4 to Fig. 5.6. Figure 5.7 demonstrated that the model responds well to periodic applications of the brake pedal.

BIBLIOGRAPHY

- [1] S. F. Williams and R. R. Knipling, "Automatic slack adjusters for heavy vehicle air brake systems," Research Report DOT HS 807 724, National Highway Traffic Safety Administration, Washington, D.C., February 1991.
- [2] R. W. Radlinski, "Braking performance of heavy U.S. vehicles," SAE Paper 870492, 1987.
- [3] "TIFA statistics," <http://www.umtri.umich.edu/cnts/doc/TIFA1999.pdf>, 2003 [Accessed January 2003].
- [4] "Inspection statistics," <http://www.nts.gov/publicctn/2002/SR0201.pdf>, 2003 [Accessed January 2003].
- [5] G. W. Stearns, "FMVSS 121 - Air brake systems: How it affects tractor-trailer combinations," *Automotive Engineering*, vol. 81, pp. 37–48, September 1973.
- [6] S. J. Shaffer and G. H. Alexander, "Commercial vehicle brake testing - Part 1: Visual inspection versus performance-based test," SAE Paper 952671, 1995.
- [7] R. M. Braswell, J. F. Broder, P. J. Fisher, R. D. Flesher, D. Foster, S. Gooch, K. F. Johnson, H. T. Pannella, R. L. Rak, G. H. Rood, J. Salas, C. O. Summer, V. Suski and J. Thrift, "Tomorrow's trucks: A progress review and reappraisal of future needs," SAE Paper 932975, 1993.
- [8] R. W. Radlinski, "Heavy vehicle braking - U.S. versus Europe," SAE Paper 892504, 1989.
- [9] M. Druzhinina, L. Moklegaard and A. G. Stefanopoulou, "Identification and integration of commercial heavy vehicle retarders," Research Report UCB-ITS-PRR-2002-14, California PATH Program, University of California, Berkeley, California, March 2002.
- [10] K. Newton, W. Steeds and T. K. Garrett, *The Motor Vehicle*, 12th edition, Warrendale, Pennsylvania: Society of Automotive Engineers, Inc., 1996.
- [11] J. C. Gerdes and J. K. Hedrick, "Brake system modeling for simulation and control," *Journal of Dynamic Systems, Measurement and Control*, vol. 121, pp. 496–503, September 1999.
- [12] Y. Khan, P. Kulkarni and K. Youcef-Toumi, "Modeling, experimentation and simulation of a brake apply system," *Journal of Dynamic Systems, Measurement and Control*, vol. 116, pp. 111–122, March 1994.
- [13] L. Johnson, P. S. Fancher and T. D. Gillespie, "An empirical model for the prediction of the torque output of commercial vehicle air brakes," Research Report UM-HSRI-78-53, Highway Safety Research Institute, University of Michigan, Ann Arbor, Michigan, December 1978.

- [14] T. M. Post, P. S. Fancher and J. E. Bernard, "Torque characteristics of commercial vehicle brakes," SAE Paper 750210, 1975.
- [15] P. G. Reinhall and R. R. Scheibe, "Development of an intelligent air brake warning system for commercial vehicles," Research Report ITS-13, IDEA Program, Transportation Research Board, National Research Council, Washington, D.C., May 1996.
- [16] S. J. Shaffer and G. H. Alexander, "Commercial vehicle brake testing - Part 2: Preliminary results of performance-based test program," SAE Paper 952672, 1995.
- [17] T. Acarman, U. Ozguner, C. Hatipoglu and A. M. Igusky, "Pneumatic brake system modeling for systems analysis," SAE Paper 2000-01-3414, 2000.
- [18] R. J. Morse, "Brake system performance at low operating pressures," SAE Paper 700512, 1970.
- [19] L. C. Buckman, "Commercial vehicle braking systems: Air brakes, ABS and beyond," paper presented at International Truck & Bus Meeting & Exposition, Society of Automotive Engineers, Indianapolis, November 1998.
- [20] D. Middleton and J. Rowe, "Feasibility of standardized diagnostic device for maintenance and inspection of commercial motor vehicles," *Transportation Research Record*, vol. 1560, pp. 48–56, 1996.
- [21] A. V. Oppenheim and R. W. Schaffer, *Digital Signal Processing*, Englewood Cliffs, New Jersey: Prentice-Hall, Inc., 1975.
- [22] B. W. Anderson, *The Analysis and Design of Pneumatic Systems*, New York: John Wiley & Sons, Inc., 1967.
- [23] H. W. Liepmann and A. Roshko, *Elements of Gasdynamics*, Mineola, New York: Dover Publications, Inc., 2001.
- [24] M. J. Zucrow and J. D. Hoffman, *Gas Dynamics*, vol. 1, New York: John Wiley & Sons, Inc., 1976.